J|A|C|S ARTICLES

Published on Web 06/03/2009

Catalyzing Racemizations in the Absence of a Cofactor: The Reaction Mechanism in Proline Racemase

Amir Rubinstein and Dan Thomas Major*

Department of Chemistry and the Lise Meitner-Minerva Center of Computational Quantum Chemistry, Bar-Ilan University, Ramat-Gan 52900, Israel

Received January 30, 2009; E-mail: majort@mail.biu.ac.il

Abstract: The origin of the catalytic proficiency of the cofactor-independent enzyme proline racemase (ProR) has been investigated by a combined classical and quantum simulation approach with a hybrid quantum mechanics/molecular mechanics potential energy surface. The present study shows that the ProR reaction mechanism is asynchronous concerted with no distinct intermediate. Various mechanisms are investigated, and it is concluded that active site residues other than the Cys dyad are not involved in chemical catalysis. When compared to an analogous aqueous solution-phase reaction, we find that the free-energy barrier is reduced by 14 kcal/mol in ProR, although the reaction mechanisms in the enzyme and in water are similar. The computed catalytic effect is comparable to that in the isofunctional enzyme alanine racemase (AlaR). However, in AlaR the catalytic burden is divided between the cofactor pyridoxal 5′-phosphate and the enzyme environment, whereas in ProR it is borne entirely by the enzyme environment. This is ascribed to a highly preorganized active site facilitating transition state stabilization via a tight network of hydrogen bonds donated by nearby active site residues.

Introduction

The abstraction of the Cα-hydrogen of amino acids poses a great challenge due to their low acidity. Typically, the pK_a values in solution of the amino acid Cα-hydrogens are in the range 21−34, depending on the nature of specific amino acid and the pH of the solution.[1] Several enzymes employ the pyridoxal-5′-phosphate (PLP) coenzyme to increase the acidity of the Cα hydrogen.[2−4] The amino acid couples with PLP via a Schiff base link, forming an aldimine moiety which has a reduced Cα pK_a value in the range of 6−17, depending on the protonation state of the PLP moiety.[5,6] This strategy is adopted by racemases such as alanine racemase (AlaR), arginine racemase (ArgR), and serine racemase (SerR). PLP is also employed by enzymes catalyzing decarboxylations, transaminations, β-eliminations, and retro-aldol cleavages. The effect of the PLP moiety is usually ascribed to a combination of factors ranging from electron sink, yllide, or solvation effects.[6−13] As evident from experiments[5−9] and computations,[10−13] the PLP cofactor is a very potent catalyst, in solution and when embedded in an enzyme environment. For instance, in the case of AlaR the Cα acidity of Ala is reduced by 13 pK_a units by the PLP moiety, and the enzyme provides an additional lowering of 7 pK_a units.[13] In light of the potency of the PLP unit as a cofactor, it is of great interest to understand the catalytic function of enzymes performing similar tasks to the PLP-dependent enzymes, but in the absence of a cofactor. Clearly, in these cases the catalytic requirements of the enzyme environment are considerably greater than in the case of PLP-dependent enzymes. Importantly, the D-form of several amino acids is required in the synthesis of the peptidoglycan layer encapsulating the cell wall in Gram-positive and -negative bacteria. Additionally, D-amino acids serve as neurotransmitters in mammalian brains.[14] Therefore, racemases present attractive targets in drug-design.

Proline racemase (ProR)[15] has been considered a prototype PLP-independent racemase, as it catalyzes the L-to-D isomerization without the aid of a cofactor. ProR belongs to a class of enzymes which also includes aspartate racemase (AspR) and glutamate racemase (GluR), as well as diaminopimelate epimerase (DAPE).[16] These proteins employ a two-base strategy with a Cys dyad serving as the acid−base pair. Interestingly, ProR is structurally more closely related to DAPE than to AspR and GluR.[16] It has been suggested that the Cα acidity in these proteins is increased by a series of strong hydrogen bonds forming a tightly bound transition state.[17] Thus, the enzyme environment is preorganized in an optimal manner for transition-

(1) Tanner, M. E. *Acc. Chem. Res.* **2002**, *35*, 237–246.
(2) John, R. A. *Biochim. Biophys. Acta* **1995**, *1248*, 81–96.
(3) Eliot, A. C.; Kirsch, J. F. *Annu. Rev. Biochem.* **2004**, *73*, 383–415.
(4) Toney, M. D. *Arch. Biochem. Biophys.* **2005**, *433*, 279–287.
(5) Dixon, J. E.; Bruice, T. C. *Biochemistry* **1973**, *12*, 4762–4766.
(6) Toth, K.; Richard, J. P. *J. Am. Chem. Soc.* **2007**, *129*, 3013–3021.
(7) Rios, A.; Amyes, T. L.; Richard, J. P. *J. Am. Chem. Soc.* **2000**, *122*, 9373–9385.
(8) Rios, A.; Crugeiras, J.; Amyes, T. L.; Richard, J. P. *J. Am. Chem. Soc.* **2001**, *123*, 7949–7950.
(9) Rios, A.; Richard, J. P.; Amyes, T. L. *J. Am. Chem. Soc.* **2002**, *124*, 8251–8259.
(10) Bach, R. D.; Canepa, C.; Glukhovtsev, M. N. *J. Am. Chem. Soc.* **1999**, *121*, 6542–6555.
(11) Toney, M. D. *Biochemistry* **2001**, *40*, 1378–1384.
(12) Major, D. T.; Nam, K.; Gao, J. *J. Am. Chem. Soc.* **2006**, *128*, 8114–8115.
(13) Major, D. T.; Gao, J. *J. Am. Chem. Soc.* **2006**, *128*, 16345–16357.
(14) Yoshimura, T.; Goto, M. *FEBS J.* **2008**, *275*, 3527–3537.
(15) Stadtman, T. C.; Elliott, P. *J. Biol. Chem.* **1957**, *228*, 983–997.
(16) Pillai, B.; Cherney, M. M.; Diaper, C. M.; Sutherland, A.; Blanchard, J. S.; Vederas, J. C.; James, M. N. G. *Proc. Nat. Acad. Sci. U.S.A.* **2006**, *103*, 8668–8673.
(17) Buschiazzo, A.; Goytia, M.; Schaeffer, F.; Degrave, W.; Shepard, W.; Grégoire, C.; Chamond, N.; Cosson, A.; Berneman, A.; Coatnoan, N.; Alzari, P. M.; Minoprio, P. *Proc. Nat. Acad. Sci. U.S.A.* **2006**, *103*, 1705–1710.

Scheme 1. Possible Reaction Mechanisms for Proline Racemase

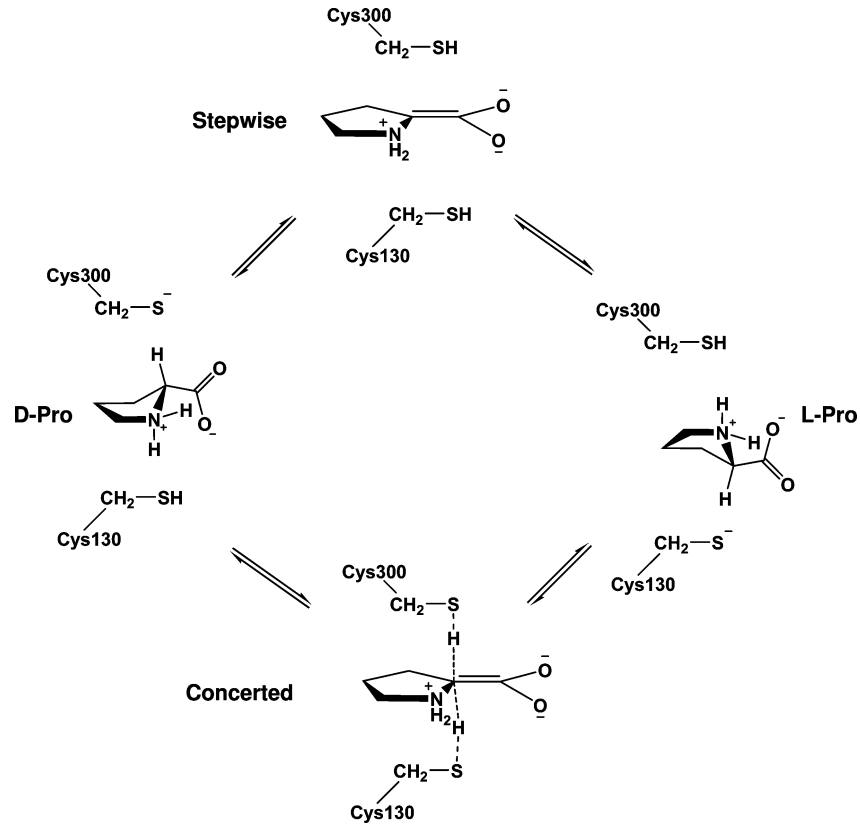

state stabilization.[18] However, in the case of ProR[19,20] and the MurI form of GluR,[21−23] it has been suggested that a protonation of the neighboring carboxylate might be required for catalysis, although no consensus exists.[24] Indeed, recent studies of GluR do not suggest protonation of the carboxylate, albeit employing different protonation states of key active site residues.[25,26]

To address the question of the Cα acidity in a non-PLP-dependent enzyme, the current study focuses on ProR, which interchanges the D and L isomers. The simplest mechanistic scheme, which we will term the *classical mechanism*, is shown in Scheme 1. In a series of groundbreaking papers by Albery, Knowles (AK), and co-workers on ProR, the energetic facets of the reaction were investigated for the protein from *Clostridium sticklandii* (*Cs*-ProR).[27−35] It was suggested that the reaction proceeds in an asynchronous manner with a proposed carbanion intermediate. Moreover, the first order rate constant, k_{cat}, was estimated to be 2600 s^{-1}.[29] The corresponding aqueous solution rate constant, k_{OH}, is 4.5 × 10^{-11} s^{-1},[20] yielding a rate enhancement of nearly 14 orders of magnitude. Thus, ProR may be considered among the most powerful enzymes in nature.[36] Additionally, proline possesses an estimated aqueous solution pK_a for the Cα-proton of ca. 29,[20] which presents a considerable thermodynamic barrier.

The first eukaryotic ProR was identified in human parasite *Trypanosoma cruzi* (*Tc*) by Reina-San-Martin et al.[37] *Tc* causes the tropical Chagas disease in mammals and is transmitted by blood-sucking assassin bugs. *Tc*-ProR is likely to play a central role in the parasite metabolism, and thus presents a potent target for chemotherapy of Chagas disease.[38,39] Additionally, ProR is likely to be present in several other pathogens of medical and agricultural interest, while absent in mammals.[40] Recently, the crystal structure of *Tc*-ProR was solved in the presence of the

(18) Warshel, A.; Sharma, P. K.; Kato, M.; Xiang, Y.; Liu, H.; Olsson, M. H. M. *Chem. Rev.* **2006**, *106*, 3210–3235.
(19) Richard, J. P.; Amyes, T. L. *Bioorg. Chem.* **2004**, *32*, 354–366.
(20) Williams, G.; Maziarz, E. P., III; Amyes, T. L.; Wood, T. D.; Richard, J. P. *Biochemistry* **2003**, *42*, 8354–8361.
(21) Puig, E.; Garcia-Viloca, M.; González-Lafont, À.; López, I.; Daura, X.; Lluch, J. M. *J. Chem. Theory Comput.* **2005**, *1*, 737–749.
(22) Puig, E.; Garcia-Viloca, M.; González-Lafont, À.; Lluch, J. M. *J. Phys. Chem. A* **2006**, *110*, 717–725.
(23) Puig, E.; Garcia-Viloca, M.; González-Lafont, À.; Lluch, J. M.; Field, M. J. *J. Phys. Chem. B* **2007**, *111*, 2385–2397.
(24) Möbitz, H.; Bruice, T. C. *Biochemistry* **2004**, *43*, 9685–9694.
(25) Puig, E.; Mixcoha, E.; Garcia-Viloca, M.; González-Lafont, À.; Lluch, J. M. *J. Am. Chem. Soc.* **2009**, *131*, 3509–3521.
(26) Spies, M. A.; Reese, J. G.; Dodd, D.; Pankow, K. L.; Blanke, S. R.; Baudry, J. *J. Am. Chem. Soc.* **2009**, *131*, 5274–5284.
(27) Cardinale, G. J.; Abeles, R. H. *Biochemistry* **1968**, *7*, 3970–3978.
(28) Rudnick, G.; Abeles, R. H. *Biochemistry* **1975**, *14*, 4515–4522.
(29) Fisher, L. M.; Albery, W. J.; Knowles, J. R. *Biochemistry* **1986**, *25*, 2529–2537.
(30) Fisher, L. M.; Albery, W. J.; Knowles, J. R. *Biochemistry* **1986**, *25*, 2538–2542.
(31) Fisher, L. M.; Belasco, J. G.; Bruice, T. W.; Albery, W. J.; Knowles, J. R. *Biochemistry* **1986**, *25*, 2543–2551.
(32) Belasco, J. G.; Albery, W. J.; Knowles, J. R. *Biochemistry* **1986**, *25*, 2552–2558.
(33) Belasco, J. G.; Bruice, T. W.; Albery, W. J.; Knowles, J. R. *Biochemistry* **1986**, *25*, 2558–2564.
(34) Belasco, J. G.; Bruice, T. W.; Fisher, L. M.; Albery, W. J.; Knowles, J. R. *Biochemistry* **1986**, *25*, 2564–2571.
(35) Albery, W. J.; Knowles, J. R. *Biochemistry* **1986**, *25*, 2572–2577.
(36) Wolfenden, R.; Snider, M. J. *Acc. Chem. Res.* **2001**, *34*, 938–945.
(37) Reina-San-Martín, B.; Degrave, W.; Rougeot, C.; Cosson, A.; Chamond, N.; Cordeiro-Da-Silva, A.; Arala-Chaves, M.; Coutinho, A.; Minoprio, P. *Nat. Med.* **2000**, *6*, 890–897.
(38) Tonelli, R. R.; Silber, A. M.; Almeida-de-Faria, M.; Hirata, I. Y.; Colli, W.; Alves, M. J. M. *Cell. Microbiol.* **2004**, *6*, 733–741.
(39) Chamond, N.; Goytia, M.; Coatnoan, N.; Barale, J. C.; Cosson, A.; Degrave, W. M.; Minoprio, P. *Mol. Microbiol.* **2005**, *58*, 46–60.

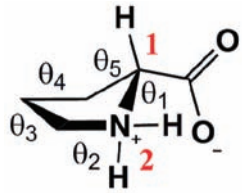

Figure 1. Proline with characteristic dihedral angles defined by sequential ring atoms.

transitions state (TS) analogue pyrrole-2-carboxylic acid (PYC), and the presence of the catalytic Cys dyad was confirmed.[17] The authors proposed a reaction mechanism in which the optimally located Cys residues in turn abstract a proton on the re-side and reprotonate from the si-side (Scheme 1). A series of tight hydrogen bonds were suggested as the source of the catalytic power of ProR. This view received support from a computational study on ProR, which presented the reaction path for the racemization.[41] However, in this case the effect of solvent was not included and no ensemble averaged free energy reaction profile was obtained, which is essential for treatment of enzymatic reactions.[42] In particular, a strategy which accounts for the conformational flexibility of proline (Figure 1) is important to correctly treat the ProR reaction.[43] Moreover, the catalytic effect of the enzyme was not elucidated by a direct comparison between the enzymatic reaction and a model reaction in aqueous solution. Finally, the question of the possible catalytic role of additional amino acid residues other than the Cys catalytic pair has yet to be addressed. Thus, principle questions regarding the reaction mechanism and the catalytic effect in ProR remain unresolved.

Here, we present the first free energy simulation of a PLP-independent racemase. The reaction mechanism in ProR is addressed via a combined classical mechanics (CM) and quantum mechanics (QM) approach. The potential of mean force (PMF) of ProR is obtained from classical umbrella sampling molecular dynamics (MD) simulations with a hybrid QM and molecular mechanics (QM/MM) potential. The enzymatic reaction is compared with an analogues reaction in aqueous solution to elucidate the catalytic power of ProR. Additionally, the question of whether the ProR reaction proceeds via a stepwise or concerted reaction mechanism is addressed by two-dimensional PMF simulations. The role of amino acid residues other than Cys130 and Cys300 is also addressed, by investigating four possible active-site protonation schemes, corresponding to different mechanistic pathways. Moreover, the QM PMF for the most likely pathway for ProR is obtained from free energy perturbation path-integral simulations (PI-FEP/UM), and the kinetic isotope effects (KIEs) are computed. Finally, the ProR reaction is compared with the PLP-dependent AlaR reaction.

Computational Details

Model of solvated Enzyme−Coenzyme−Substrate Complex. The X-ray crystallography structure of *Tc*-ProR was recently published by Buschiazzo et al.[17] The enzyme is a homodimer comprised of two α/β units containing 414 amino acids which are separated by a deep cleft. Each monomer possesses an independent active site pocket, which is sequestered from water. Two forms of the enzyme were solved, at 2.1 and 2.5 Å resolution, respectively: one in which both actives sites are occupied by the transition-state analogue, PYC (PDB code: 1W61), and the other structure where only one active site is occupied by PYC (PDB code: 1W62). The enzyme undergoes considerable conformational change upon ligand binding, and the Cα rmsd between the two monomers in 1W62 is 2.2 Å. However, the rmsd difference between the two PYC binding units in the two crystal forms (1W61 and 1W62) is 0.3 Å, suggesting that substrate binding in one monomer has little influence on the structure of the second monomer. Thus, in both crystal structures the PYC binding monomers are very similar, and since the binding site is deeply buried within each monomer, one may chose either crystal structure for the computational work. In the current study, the highest resolution structure was employed (1W61). The overall structure of the enzyme is similar to the *Hemophilus influenzae* DAPE enzyme,[16] with 60−80% of the secondary structure elements conserved. The homology between *Tc*-ProR and *Cs*-ProR is considerable with 52.4% identity.[37] The main difference between the two proteins is the additional C- and N-terminal domains in *Tc*-ProR. Most of the residues found to be important for catalysis (see Results section below) are identical in the two homologues, suggesting very similar catalytic properties for the two enzymes.

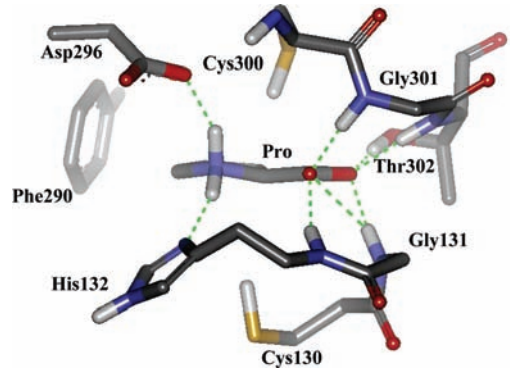

Figure 2. Active-site interactions of proline racemase with bound substrate proline in the transition state.

The catalytic residues, Cys130 and Cys300,[27] are located on opposite sides of the PYC plane, posed to serve as the acid−base pair (Figure 2).[17] The crystal structure reveals a highly preorganized and polar active site, with four amide groups (Gly131, His132, Gly301, Thr302) and the Thr302 side chain donating hydrogen bonds to the proline carboxylate. This tight network of H-bonds suggests that protonation of the proline carboxylic acid is an unlikely scenario. Additionally, the proline quaternary amine group interacts with His132 and Asp296. This stabilization of the amine, suggests that the Cys130/300 thiolates are unlikely to be inactivated by protonation due to the amine. Additionally, His132 interacts with the backbone carbonyl of Ala57 while Asp296 interacts with Ser298. On the basis of their respective hydrogen-bonding patterns and standard pK_a values, His132 is modeled in the neutral form while Asp296 is ionized. This network of interactions, which is also observed in DAPE, suggests a structural role for His132 and Asp296, rather than a chemical role.[16,17] Additional hydrophobic interactions with Phe102 and Phe290 firmly lock the substrate in place for catalysis and sequesters the active site from surrounding water molecules.

Hydrogen atoms were added to the enzyme using the HBUILD module of the CHARMM program,[44] while the hydrogen atoms of the substrate were added manually. The protonation states of all

(40) Chamond, N.; Gregoire, C.; Coatnoan, N.; Rougeot, C.; Freitas-Junior, L. H.; da Silveira, J. F.; Degrave, W. M.; Minoprio, P. *J. Biol. Chem.* **2003**, *278*, 15484–15494.
(41) Stenta, M.; Calvaresi, M.; Altoè, P.; Spinelli, D.; Garavelli, M.; Bottoni, A. *J. Phys. Chem. B* **2008**, *112*, 1057–1059.
(42) Klähn, M.; Braun-Sand, S.; Rosta, E.; Warshel, A. *J. Phys. Chem. B* **2005**, *109*, 15645–15650.
(43) Kapitán, J.; Baumruk, V.; Kopecký, V. Jr.; Pohl, R.; Boul, P. *J. Am. Chem. Soc.* **2006**, *128*, 13451–13462.
(44) Brooks, B. R.; Bruccoleri, R. E.; Olafson, B. D.; States, D. J.; Swaminathan, S.; Karplus, M. *J. Comput. Chem.* **1983**, *4*, 187–217.

Table 1. Proton Affinities (kcal/mol) for Model Compounds for the Proline Racemization by Proline Racemase

	AM1	SRP-AM1[a]	mPW91PW91[b]	exptl[c]
methanethiolate (S^-)	352.7	354.6	356.9	358 ± 2
proline (C_α)[d]	347.4 (364.8)	373.9 (380.4)	371.1 (378.2)	

[a] Reaction specific parameter AM1 from ref 12. [b] mPW91PW91/6-311++G(3df,2p)//mPW91PW91/6-31+G(d). [c] Reference 49. [d] Values for nonzwitterionic and zwitterionic (in parentheses) structures.

Table 2. Interaction Energies (kcal/mol) for Model H-Bonding Complexes Using Optimized van der Waals Parameters

donor	acceptor	SRP-AM1[a]	ab initio[b]
H_2O	methanethiol	−3.89	−2.99
methanethiol	H_2O	−2.24	−1.84
H_2O	methanethiolate	−12.88	−12.63

[a] QM/MM interaction energy using reaction specific parameter AM1 from ref 12 and TIP3P water. [b] HF/6-31+G(d)//HF/6-31+G(d).

ionizable residues were assigned on the basis of pH 8.[29] His residues were modeled as neutral or protonated moieties with hydrogen positioned either at Nδ or Nε or both, depending on their hydrogen-bonding pattern with surrounding amino acid residues or water molecules.

Potential Energy Surface. The potential energy surface (PES) in the current study is described by a hybrid QM/MM Hamiltonian.[45,46] The QM part is described by a modified AM1 semiempirical Hamiltonian,[47] where the parameters have been optimized to treat amino acid racemization reactions (specific reaction parameters, denoted SRP-AM1),[12,13] while the MM part is described by the CHARMM22 force field.[48] This combined potential energy yields accuracy comparable to density functional theory (DFT) and was shown to give accurate results for the AlaR reaction.[12,13]

To establish the accuracy of SRP-AM1 for the current proton-abstraction reaction, a model gas-phase reaction was investigated. The model reaction involved a methanethiolate anion and zwitterionic and nonzwitterionic proline. The model calculations were performed with the SRP-AM1 model and compared to experimental[49] and DFT data. The DFT method chosen was the modified PW91PW91 functional with a 6-311++G(3df,2p) basis set.[50] The model calculations revealed good accord between the SRP-AM1 Hamiltonian and the DFT results (Table 1).

To fine-tune the PES, QM/MM interaction energies between the reacting fragments (QM) and individual water molecules (MM) were investigated (Figure S1). The van der Waals (vdW) radii of the QM fragments were changed so as to minimize the error between the QM(SRP-AM1)/MM interaction energies and ab initio interaction energies at the HF/6-31+G(d) level (Table 2).[51] Only the vdW radii of the sulfur of methanethiol/methanethiolate and the oxygens of proline were optimized.

In the QM/MM approach, the region of primary interest such as the enzyme active site is treated at the QM level, while the remaining part of the system is treated at the MM level. In the current study of ProR the QM region comprises the substrate proline and the side-chains of the catalytic residues Cys130 and Cys300, including the Cα atoms. The connection between the QM and MM regions is described by the generalized hybrid orbital (GHO) method.[52,53] For the model reaction in aqueous solution phase, the QM region consisted of methanethiolate and zwitterionic proline. Water molecules were described by the three point charge TIP3P model.[54]

Stochastic Boundary MD. The current MD study employed stochastic boundary conditions for the enzymatic reaction due to the size of ProR.[55] The temperature of the simulations was 310 K.[29] The simulations employed the Leap-Frog integration scheme with a time step of 1 fs.[56] TIP3P water hydrogens were constrained using the SHAKE algorithm.[56] The nonbonded interactions were set to zero at distances beyond 14 Å. The electrostatic forces were shifted to zero from a distance of 12 Å, while the vdW interaction energy was switched to zero at 12 Å.

Aqueous Solution-Phase Model Simulations. An aqueous solution-phase model reaction mimicking the proton abstraction in ProR was investigated. The reaction involved a methanethiolate ion as a base, which abstracts the C_α-proton from proline embedded in TIP3P water and including a sodium ion to neutralize the system. The L-isomer form of proline was used. The simulations used periodic boundary conditions with electrostatics treated by the Ewald summation method.[57] The center-of-mass of the reacting supermolecule was placed at the center of a cubic box of dimensions $33 \times 33 \times 33$ Å^3. The solution-phase reaction was performed using the constant particle−pressure−temperature (NPT) ensemble at 298 K and 1 atm.[58] The simulations employed the Leap-Frog integration scheme with a time step of 1 fs, and TIP3P water hydrogens were constrained with SHAKE algorithm.[56]

Free Energy Simulations. The classical PMF as a function of the reaction coordinate was defined as

$$W^{\mathrm{cl}}(z) = -RT \ln \rho(z) + C \qquad (1)$$

where ρ is the unbiased probability density along the reaction coordinate z, R is the gas phase constant, T is the temperature, and C is an arbitrary constant.[59] For the model aqueous solution-phase reaction, the reaction coordinate was defined as the difference between the breaking C_α−H bond and forming S−H bond. For the ProR reaction the reaction coordinate was defined by two independent reaction coordinates, z_1 and z_2. Here z_1 is defined as the difference between the breaking C_α−H bond and forming S_{C130}−H bond, $z_1 = R(C_\alpha\text{−H}) - R(S_{Cys130}\text{−H})$, while z_2 is defined as the difference between the forming C_α−H bond and breaking S_{C300}−H bond, $z_2 = R(C_\alpha\text{−H}) - R(S_{Cys300}\text{−H})$. The free energy of the ProR reaction was modeled employing a two-dimensional free-energy strategy,[60] wherein the PMF is defined as

$$W^{\mathrm{cl}}(z_1, z_2) = -RT \ln \rho(z_1, z_2) + C \qquad (2)$$

The minimum free-energy path on the two-dimensional PMF surface was obtained by following the steepest descent path from the transition state on the free-energy surface. This was done by computing numerical derivatives of the two-dimensional PMF surface.

(45) Gao, J. In *Reviews in Computational Chemistry*; Lipkowitz, K. B., Boyd, D. B., Eds.; VCH: New York, 1995; Vol. 7, pp 119−185.
(46) Gao, J.; Thompson, M. A. *Combined Quantum Mechanical and Molecular Mechanical Methods*; American Chemical Society: Washington, DC, 1998; Vol. 712.
(47) Dewar, M. J. S.; Zoebisch, E. G.; Healy, E. F.; Stewart, J. J. P. *J. Am. Chem. Soc.* **1985**, *107*, 3902–3909.
(48) MacKerell, Jr, A. D.; et al. *J. Phys. Chem. B* **1998**, *102*, 3586–3616.
(49) Schwartz, R. L.; Davico, G. E.; Lineberger, W. C. *J. Electron Spectrosc. Relat. Phenom.* **2000**, *108*, 163–168.
(50) Adamo, C.; Barone, V. *J. Chem. Phys.* **1998**, *108*, 664–675.
(51) Hehre, W. J.; Radom, L.; Schleyer, P. v. R.; Pople, J. A. *Ab Initio Molecular Orbital Theory*; John Wiley and Sons: New York, 1986.
(52) Gao, J.; Amara, P.; Alhambra, C.; Field, M. J. *J. Phys. Chem. A* **1998**, *102*, 4714–4721.
(53) Amara, P.; Field, M. J.; Alhambra, C.; Gao, J. *Theor. Chem. Acc.* **2000**, *104*, 336–343.
(54) Jorgensen, W. L.; Chandrasekhar, J.; Madura, J. D.; Impey, R. W.; Klein, M. L. *J. Chem. Phys.* **1983**, *79*, 926–935.
(55) Brooks III, C. L.; Brünger, A.; Karplus, M. *Biopolymers* **1985**, *24*, 843–865.
(56) Allen, M. P.; Tildesley, D. J. *Computer Simulation of Liquids*; Oxford University Press: Oxford, U.K., 1987.
(57) Nam, K.; Gao, J.; York, D. M. *J. Chem. Theory Comp.* **2005**, *1*, 2–13.
(58) Feller, S. E.; Zhang, Y.; Pastor, R. W.; Brooks, B. R. *J. Chem. Phys.* **1995**, *103*, 4613–4621.
(59) Kottalam, J.; Case, D. A. *J. Am. Chem. Soc.* **1988**, *110*, 7690–7697.
(60) Rajamani, R.; Naidoo, K. J.; Gao, J. *J. Comput. Chem.* **2003**, *24*, 1775–1781.

Practically, the PMF was obtained by employing adaptive umbrella sampling MD simulations,[61] combined with the weighed histogram analysis method (WHAM).[62]

In the current study, the systems were slowly heated to the target temperature over the course of 25 ps, followed by ca. 0.5 ns of equilibration. Thereafter, to obtain the two-dimensional PMF, the reaction coordinates were divided into 12 windows each, yielding 72 windows spanning the upper diagonal of the two-dimensional surface. For the model reaction in water the reaction coordinate was divided into ca. 30 windows. Each window was further equilibrated for 100−150 ps and sampled for 200 ps. Thus, the total simulation of the classical mechanism in ProR lasted for ca. 24 ns, for the additional ProR mechanisms ca. 6 ns, and for the model reaction ca. 10 ns.

Nuclear Quantum Mechanical Effects. Nuclear quantum mechanical effects (NQE) are not included in the PMF obtained from classical MD simulations. These effects are required to obtain accurate rate constants in proton transfer reactions, as well as for computation of KIEs. In the current work, we employ centroid path integral (PI) simulations[63−65] to evaluate the QM potential of mean force for the proline racemase reaction. In particular, we employ the bisection sampling scheme (BQCP), where we utilize the fact that the exact free particle distribution is known and path integral configurations can be sampled independently, yielding rapid convergence.[63,64] Moreover, we have developed a mass perturbation scheme for computing accurate free-energy difference of isotope substitutions, needed for prediction of KIE (PI-FEP/UM).[65]

In the PI simulation, we represent each quantized atom by a ring of quasi-particles or beads, wherein their geometrical center (centroid) is constrained to the classical position. Thus, for a classical configuration sampled in MD umbrella sampling simulations, PI sampling is performed to obtain the correction for NQE.

In the present study, we used 32 beads for each of the quantized atoms (donor and acceptor heavy atoms, namely S_{130}, S_{300}, and Cα, transferring protons, as well as all other heavy atoms of the substrate). Previous studies have shown that this treatment yields good convergence in the overall quantum corrections for model proton transfer reactions in water.[64] BQCP simulations were performed on classical configurations along the PMF reaction coordinate, at the temperature employed in the classical simulations. For the ProR reaction, the BQCP simulations were performed in the vicinity the CM minimum free-energy path on the two-dimensional surface, and a refined QM minimum free energy path was obtained. For the solution-phase reaction, 57 200 configurations were extracted from the MD trajectory, while for the ProR reaction, 90 800 were extracted. Each of these MD frames was sampled by 10 free particle steps for H and D substitution to obtain the quantum corrections. For the solution-phase reaction, the QM correction along the entire reaction path was represented by an inverse one-dimensional asymmetric Eckart potential fitted via nonlinear Levenberg−Marquardt minimization. For the ProR reaction, the QM correction was represented by a cubic two-dimensional surface which was added to the PMF surface.

Electrostatic Interaction Analysis of ProR. Structures saved during the umbrella sampling-MD simulations of ProR were employed to analyze the contribution of individual residues to transition state stabilization (see Supporting Information). Trajectory structures corresponding to the stationary points along the reaction coordinate (±0.1 Å), namely reactant state (RS), transition state (TS), and product state (PS), were extracted for further analysis. These three states are defined by the sets of abscissa/ordinate defining states on the two-dimensional PMF (z_1,z_2). The RS is defined at (−0.7, 1.8) corresponding to L-Pro, TS at (0.8, 0.7), and PS at (1.6, −0.7) corresponding to D-Pro. A total of ca. 1000−3000 configurations were averaged for each of the RS, TS, and PS states.

Proline Pseudorotation Analysis. The conformation of the five-membered ring in proline was characterized by the puckering phase, P, and the puckering amplitude, θ_m, which where defined as follows[43]

$$\tan(P) = \frac{\theta_3 + \theta_5 - \theta_2 - \theta_4}{2\theta_1[\sin(\pi/5) + \sin(2\pi/5)]} \quad (3)$$

$$\theta_m = \theta_1/\cos(P) \quad (4)$$

The angles θ_i $i = 1-5$ are defined in Figure 1. The conformational analysis was performed for the aqueous solution and enzymatic reactions at the RS, TS, and PS employing ca. 5000 frames from the MD simulations.

All gas-phase QM calculations employed the Gaussian 03 program,[66] while all QM/MM calculations and simulations employed the CHARMM program.[44]

Results

Model Gas-Phase Reactions. Ab Initio and Semiempirical Calculations. In Table 1 the computed proton affinities of the C_α-proton in proline, as well as for methanethiol, are presented. These model reactions show that the SRP-AM1 model developed for the AlaR reaction is equally applicable to the ProR reaction. The proton affinity for methanethiol is 354.6 kcal/mol at the SRP-AM1 level, while it is 356.9 kcal/mol at the DFT level and 358 ± 2 from experiment.[49] For zwitterionic proline the SRP-AM1 proton affinity is 380.4 kcal/mol comparable to 378.2 at the DFT level, while the nonzwitterionic form the respective values are 373.9 and 371.1 kcal/mol at the SRP-AM1 and DFT levels.

QM/MM Calculations. To fine-tune the QM/MM interactions between a quantum mechanical Cys and the surrounding environment, which is treated by molecular mechanics, model complexes with water molecules were constructed (Figure S1). Two complexes of methanethiol and one complex of methanethiolate, each with a water molecule, were computed at ab initio and QM/MM level, while optimizing the vdW radius of the sulfur atom (Figure S1 and Table 2). The TIP3P model was used as MM water. The average unsigned error for the three complexes with the optimized vdW radius ($\sigma = 4.50$ Å, $\varepsilon = -0.65$ kcal/mol) was 0.5 kcal/mol. For the remaining QM atoms, standard QM/MM vdW parameters were employed; for the proline carboxylate oxygens, an intermediate value between sp^3 and sp^2 oxgens was employed ($\sigma = 2.50$ Å, $\varepsilon = -0.40$ kcal/mol).[67]

Aqueous Solution-Phase Model Reaction Potential of Mean Force Simulations. To determine the catalytic effect of ProR it is essential to have a detailed understanding of the corresponding aqueous solution phase reaction. To this end, the relative free energies and pK_a values were obtained from a series of MD simulations employing umbrella sampling. The proton abstraction reaction of proline zwitterion by methanethiolate, serves as a model for the enzymatic reaction where a deprotonated Cys residue abstracts the Cα-proton from proline and an antipodal Cys residue reprotonates the carbanion to generate the other enantiomer. Furthermore, such a calculation provides validation of the potential energy functions and free energy

(61) Torrie, G. M.; Valleau, J. P. *J. Comp. Phys.* **1977**, *23*, 187–199.
(62) Kumar, S.; Bouzida, D.; Swendsen, R. H.; Kollman, P. A.; Rosenberg, J. M. *J. Comput. Chem.* **1992**, *13*, 1011–1021.
(63) Major, D. T.; Gao, J. *J. Mol. Graph. Mod.* **2005**, *24*, 121–127.
(64) Major, D. T.; Garcia-Viloca, M.; Gao, J. *J. Chem. Theory Comp.* **2006**, *2*, 236–245.
(65) Major, D. T.; Gao, J. *J. Chem. Theory Comput.* **2007**, *3*, 949–960.
(66) Frisch, M. J.; et al. *Gaussian 03, revision D.02*; Gaussian, Inc.: Pittsburgh, PA, 2003.
(67) Gao, J.; Xia, X. *Science* **1992**, *258*, 631–635.

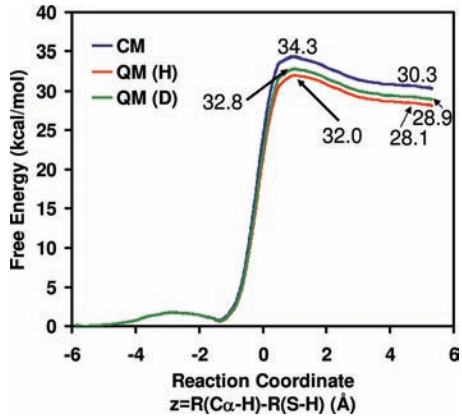

Figure 3. Computed classical and quantum potentials of mean force for proton abstraction reaction of proline and a methanethiolate ion in water.

Table 3. Free Energies of Reaction and Activation (kcal/mol) and KIEs for the Deprotonation of Proline by Methanethiolate in Aqueous Solution and by ProR

	ΔG^{reac}_{cm}	$\Delta G^{reac\,a}_{qm}$	exptl	$\Delta G^{\ddagger}_{cm}$	$\Delta G^{\ddagger\ a}_{qm}$	exptl	KIE	exptl
CH_3S^-	30.3	28.1	25.5[b]	34.3	32.0	31.6[d]	3.9	
ProR	0.7	0.7	0.0[c]	20.5	18.6	13.3[e]	3.0	2.66[f]

[a] Transferring isotope was H. [b] References 20 and 68. [c] References 29 and 34. [d] Reference 20. [e] Reference 29. [f] Reference 31.

simulation methods used in the enzymatic reactions. The computed free energy profile in water for the proton abstraction of proline by methanethiolate is shown in Figure 3, and the results are summarized in Table 3.

For the uncatalyzed deprotonation of proline by methanethiolate ion in water, we obtained a classical free-energy barrier of 34.3 kcal/mol. Addition of NQE reduces this barrier to 32.0 kcal/mol for proton transfer, which may be compared to the experimental value of 31.6 kcal/mol where the base is OH^-.[20] In the case of deuteron transfer, the free energy barrier is 32.8 kcal/mol, yielding a predicted KIE of 3.9. The classical reaction free energy is 30.3 kcal/mol using the SRP-AM1 potential. Addition of NQE yields a free energy of 28.1 kcal/mol, which is slightly greater than experiment (25.5 kcal/mol), based on pK_a values for proline (29)[20] and methanethiol (10.3).[68] The computed pK_a for proline, based on the PMF and the experimental value for methanethiol, is 30.9. Figure 3 shows that spontaneous proton exchange is extremely disfavored thermodynamically in aqueous solution at 25 °C and the observation of a stable carbanion species in water is highly unlikely.

ProR Potential of Mean Force Simulations of the Classical Mechanism. The simplest mechanism for ProR isomerization of L-Pro to D-Pro entails the Cys130/Cys300 dyad in the thiolate/thiol forms, respectively, while His132 and Asp296 are in their neutral and carboxylate forms respectively. In this scheme (Scheme 1) Cys130 is deprotonated either by a water molecule or an initially neutral form of the amine moiety of the substrate. Thus, His132 and Asp296 do not serve a catalytic acid−base role in the racemization step but interact tightly with the ammonium moiety of the substrate (Figure 2).

The computed classical and quantum mechanical two-dimensional potentials of mean force for the Pro racemization

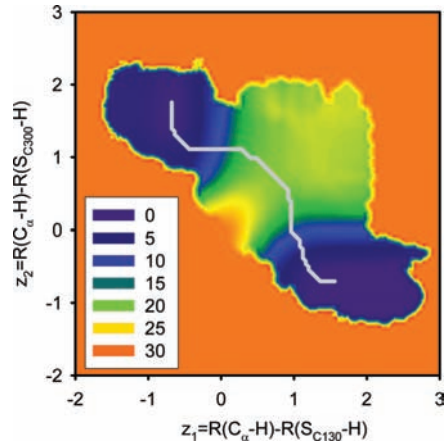

Figure 4. Computed classical two-dimensional potential of mean force for the proton abstraction of L-Pro by Cys130, and the reprotonation of proline carbanion by Cys300 in ProR.

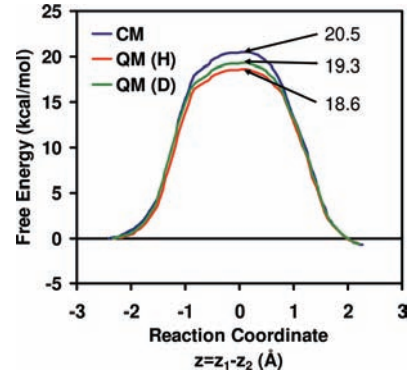

Figure 5. Computed CM and QM minimum free-energy paths on the two-dimensional potential of mean force surfaces for the proton abstraction of L-Pro by Cys130 and the reprotonation of proline carbanion intermediate by Cys300 in ProR.

reaction (Scheme 1), both for proton transfer and deuteron transfer, catalyzed by ProR are depicted in Figures 4, 5, S2, and S3. The ProR catalytic cycle involves two proton-transfer reactions in either direction of the racemization. In the L-to-D direction, Cys130 thiolate ion abstracts the C_α-proton to yield a carbonanion, which is followed by a proton transfer from Cys300 to form D-Pro (Scheme 1). The reaction coordinate for the first proton-transfer step, z_1, which is defined as the difference in bond length between $C_\alpha-H$ and $H-S_{Cys130}$, corresponds to the *x*-axis. Similarly, the reaction coordinate for the second proton transfer step, z_1, is defined as the difference between $S_{Cys300}-H$ and $H-C_\alpha$, and corresponds to the *y*-axis. By this definition, in Figures 4, S2, and S3 the reactant state involving L-Pro is located in the upper left corner while the product state involving D-Pro is located in the lower right corner of the two-dimensional PMF contour map.

The PMF for the ProR reaction is in good qualitative agreement with the free-energy reaction profile deduced from experimental kinetic data by AK.[34] The overall free energy of reaction for the classical PMF is 0.7 kcal/mol for the conversion from L- to D-Pro. Considering the identical k_{cat} values for the catalytic steps in the L→D and D→L directions obtained by AK, this is an indication of the accuracy of the current PES, as well as the lack of hysteresis in the simulations. The minimium free energy path is indicated on the two-dimensional map in Figures 4, S2, and S3. This path indicates that the reaction mechanism is concerted, yet asynchronous, in agreement with the results

(68) Serjeant, E. P.; Dempsey, B., Eds. *Ionization Constants of Organic Acids in Solution, IUPAC Chemical Data Series No. 23*; Pergamon Press: Oxford, U.K., 1979.

of AK and Stenta et al.[41] Furthermore, inspection of the free-energy surface reveals that no stable intermediate is formed. This is similar to the mechanism found for the racemization of zwitterionic Pro in water. Thus, there is no change in reaction mechanism in going from aqueous solution to the enzyme, and in both cases, the carbanion is a transient species. Nonetheless, one may estimate an apparent pK_a value for Pro in ProR. Inspection of the PMF profile indicates an enhanced acidity in ProR by 7.5 pK_a units to a value of 23.4 (the estimated experimental pK_a of 8.0−8.5 for ProR was used,[40] which is similar to the value of 8.4 for sulfhydryl[69]).

The computed classical free energy of activation for the proton abstraction by Cys130/Cys300 thiolate ion is estimated to be 20.5 kcal/mol, while including NQE reduces this barrier to 18.6 kcal/mol in the case of the proton transfer and 19.3 kcal/mol in the case of deuteron. For comparison, the experimental value is 13.3 kcal/mol for the proton transfer.[34] The agreement with experiment is reasonable, considering the computational complexity involved in the enzymatic process and the slight underestimation of the proton affinity of methanethiolate (Table 1). The closer agreement upon inclusion of NQE reinforces previous conclusions that zero-point effects and QM tunneling, which are both included in the present path integral simulations (Figure 5), are important for computing rate constants for enzymatic reactions involving proton transfers.[70] The predicted primary KIE is 3.0 for the ProR reaction, which may be compared with the experimental value of 2.66.[31] The good agreement with experiment lends support to the combined computational strategy and the proposed mechanism.

ProR Potential of Mean Force Simulations of Alternative Mechanisms. Richard et al. have suggested carboxylate protonation as a general mechanism to enhance Cα acidity of amino acids.[7] This has also been suggested in minimization studies of GluR,[21−23] although these studies might have employed an inactive form of the enzyme.[71] More recent studies on GluR, employing the enzyme from *Bacillus subtilis* co-crystallized with D-glutamate, suggest an unprotonated carboxylate.[25,26] We have examined the possibility of carboxylate protonation in our computations, but found that the tight network of H-bonds to the Pro carboxylate is compromised in the event of protonation, due to repulsion between the carboxylic acid proton and the hydrogen-bond-donating moieties. Indeed, five tight H-bonds combined with a neighboring ammonium of Pro makes carboxylate protonation an unlikely scenario.

Additional mechanistic schemes may be envisioned for ProR. To examine these mechanisms we have performed the Cα-proton transfer steps involving Cys130/Cys300 (Scheme 1), with various protonation schemes of key active site residues. Implicit in these schemes are prior proton-transfer steps between initially neutral Cys residues and either (a) His132 (yielding a protonated His), (b) Asp296 (neutral Asp296), or (c) both (protonated His, neutral Asp296). In mechanisms 2 and 3, His132 and Asp296 serve as the general base, respectively, deprotonating Cys130 (Cys300) in the L→D (D→L) direction. In mechanism 4 both His132 and Asp296 are protonated and participate in the catalytic steps, in an analogues manner to a proposed mechanism for GluR.[25] The Cα proton transfer with the different protonation states of His132 and Asp296, correspond to the racemization step in mechanisms 2−4. Herein, we only consider the Cα deprotonation step, and do not consider proton transfers involving His132/Asp296 in concert with the racemization step.

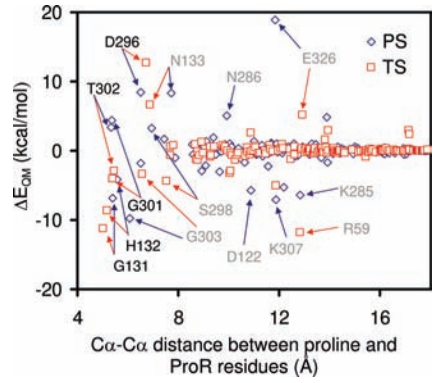

Figure 6. Individual residue contribution to stabilization or destabilization of the TS (red squares) and PS (blue diamonds) relative to the reactant state (the L-Pro Michaelis complex in proline racemase) as a function of the distance between the C_α atoms of L-Pro and residues. Residue names in black indicate those that form hydrogen-bonding interactions with proline, Cys130 or Cys300, and residue names in gray do not have direct contact with the QM region.

Inspection of the free energy profiles for mechanisms 2−4 clearly suggests that these are unlikely scenarios. The free-energy barriers are higher than the classical mechanism by 18, 11, and 8 kcal/mol, respectively (Figure S4). Indeed, these barriers are in qualitative disagreement with the kinetic data of AK. Further analysis of the structural data strengthens this conclusion, as key interactions observed between enzyme and the transition state inhibitor PYC are lost for mechanisms 2−4 (Tables S7−S9).

In the following analyses, only the classical mechanism will be considered.

Electrostatic and Structural Analysis. To estimate the contribution of individual residues to catalysis, an electrostatic decomposition analysis was performed as described in the Computational Details section. This analysis accounts for the electrostatic interactions between the enzyme environment which is treated by MM and the reactive QM active-site fragment which includes the substrate and the catalytic Cys residues. The results are presented in Figure 6 and show the ensemble averaged contribution of each amino acid to TS and PS stabilization, relative to the RS.

The TS in ProR is stabilized by a network of strong H-bonds to the carboxylate moiety. The Thr302 side-chain donates a hydrogen bond, while the backbone amides of Gly131, His132, Gly301, and Thr302 donate additional hydrogen bonds. These latter residues stabilize the TS by 11, 9, 4, and 3 kcal/mol, respectively, relative to the reactant state. This stabilizing effect is also reflected in shortening of the hydrogen bonds as the system moves from the RS/PS to the TS (Table 4). An exception to this is Thr302 which shows a slight elongation of the hydrogen bond at the TS compared to the RS. In contrast to these residues, Asp296, which interacts with the Pro ammonium, destabilizes the TS due to repulsive electrostatic interaction with the Pro carbanion. Asn133 destabilizes the TS due to a backbone amide hydrogen-bond interaction with the Cys130 thiolate in the RS (L→D direction), which is weakened as the negative charge on the sulfur migrates to the C_α atom of Pro. A similar role is played by the Gly303 backbone amide which interacts with the Cys300 thiolate in the PS (D→L direction). This is

(69) Dawson, R. M. C.; Elliott, D. C.; Elliott, W. H.; Jones, K. M. *Data for biochemical research*, 3rd ed.; Oxford Science Publications: Oxford, U.K., 1986; pp 1−31.
(70) Gao, J.; Truhlar, D. G. *Annu. Rev. Phys. Chem.* **2002**, *53*, 467–505.
(71) Ruzheinikov, S. N.; Taal, M. A.; Sedelnikova, S. E.; Baker, P. J.; Rice, D. W. *Structure (Cambridge)* **2005**, *13*, 1707–1713.

Table 4. Average Distances (Å) for Selected Hydrogen-Bonding Interactions in the Michaelis Complex RS (L-Pro), the TS, and the Michaelis Complex PS (D-Pro), which Have Been Averaged Over 5000 Configurations[a]

donor	acceptor	RS	TS	PS
N, Gly131	OXT, Pro	2.70	2.57	2.66
N, His132	O, Pro	2.79	2.55	2.60
N, Gly301	O, Pro	2.66	2.57	2.87
N, Thr302	OXT, Pro	2.60	2.66	2.76
OG1, Thr302	OXT, Pro	2.59	2.60	2.59
N, Pro	ND1, His132	2.93	2.95	3.23
N, Pro	OD2, Asp296	3.13	2.77	2.76

[a] Standard deviations in the average distances are 0.1−0.3 Å.

reflected in the stabilization of the PS relative to the RS by Gly303 amounting to 10 kcal/mol. Additional distant residues affect TS stabilization via long-range electrostatics. Arg59 contributes 12 kcal/mol to TS stabilization, while Glu326 destabilizes the TS by 5 kcal/mol. Nonetheless, the principle catalytic effect in ProR is due to nearby residues.

The Michaelis complex reactant (L-Pro) and product (D-Pro) states are characterized by similar stabilizing interactions (Figure 6). L-Pro is stabilized mainly by amide backbone interactions donated by Gly301 and Thr302, while D-Pro is mainly stabilized by amide backbone interactions donated by Gly131 and His132. Quantitatively these differential contributions amount to a stabilization of L-Pro by 4 and 3 kcal/mol, respectively, for Gly301 and Thr302, relative to D-Pro. This conclusion is confirmed by inspection of the changes in hydrogen-bond distances in the RS and PS. The hydrogen bonds between the Pro carboxylate oxygens and Gly301 and Thr302 are 0.21 and 0.16 Å shorter in the RS than in the PS, respectively (Table 4). Conversely, Gly131 and His132 preferentially stabilize D-Pro relative to L-Pro. This is exemplified by differential electrostatic interactions of 7 and 4 kcal/mol due to Gly131 and His132, respectively. These values are supported by reduced hydrogen-bond distances between backbone amides and the Pro carboxylate of 0.04 Å for Gly131 and 0.19 Å for His132.

It is interesting to note that most of the residues mentioned in the above discussion are conserved between *Tc*-ProR and *Cs*-ProR, therefore justifying the comparison of experimental kinetic data for *Cs*-ProR[34] and the computational data obtain herein for *Tc*-ProR.

The conformational preference and flexibility of the five-membered ring in proline may be described in terms of the pseudorotation angle, P (eq 3), and the puckering amplitude, θ_m (eq 4).[43] The pseudorotation angle describes the conformation of the five-membered ring, while the amplitude describes the deviation from planarity. In the following discussion, we will define four regions of the pseudorotation cycle (range is 0−360°):[43] North (45−135°), West (135−225°), South (225−315°), and East (315−45°). All accompanying figures are included as Supporting Information. Inspection of the stationary points along the PMF for the aqueous solution-phase reaction reveals a wide distribution for the pseudorotation angle. In the RS there is a preference for the eastern hemisphere while for the TS and PS (carbanion form of proline) there is a near uniform pseudorotation distribution (Figures S5−S10). The conformational preference of the RS, which was built in the L-Pro isomeric form, is due to an intramolecular H-bond between the carboxylate and protonated amine. Interestingly, the entire pseudorotation cycle is accessible throughout the simulations. The puckering amplitude for the TS and PS are lower than for the RS, indicating a more planar ring conformation as the Cα-carbanion formation progresses (Figures S5−S10).

Examination of the stationary points along the PMF for the enzymatic reaction reveals a considerable more narrow distribution for pseudorotation angle than in the aqueous solution phase analogue (Figures S11−S16). In the RS (L-Ala) there is a preference for the northeastern hemisphere, similar to that observed for the aqueous solution phase simulation, although the distribution is considerably more peaked in ProR. For the PS (D-Ala) there is a preference for the northern hemisphere. At the TS there is a binomial distribution with peaks in the northeastern and southern hemispheres. The puckering amplitude for the TS is considerably lower than for the RS and PS, reflecting a planar ring (Figures S11−S16). Interestingly, the PS (D-Ala) has a lower amplitude than the RS (L-Ala), indicating greater strain in this state. We ascribe this strain to steric congestion due to the presence of Phe102 and Phe290, which limits the mobility of the five-membered ring atoms. In particular, Phe102 seems to preferably limit the flexibility of D-Pro. In conclusion, ProR imposes conformational restraints on the substrate to narrow regions of pseudorotational space.

Discussion

A main finding in this study is the similar reaction mechanism for the L-to-D isomerization of proline in aqueous solution phase and in the enzyme ProR. In both cases the reaction proceeds without the formation of a stable intermediate. In aqueous solution phase the carbanion intermediate was found to have a reprotonation barrier of only 4.0 kcal/mol. In ProR the reaction is suggested to go via a nonsynchronous concerted reaction path, without a distinct intermediate, in agreement with the mechanism suggested by AK.[27] This similar reaction mechanism in the uncatalyzed and ProR catalyzed reaction raises important questions regarding the catalytic burden borne by ProR in comparison with other racemase enzymes. In ProR the entire computed catalytic effect of 14 kcal/mol may be ascribed to the effect of the enzyme environment. The tight networks of H-bonds are prearranged in order to stabilize the transition state of the reaction,[72] and the enzyme requires no further aid from a cofactor. Interestingly, there are seemingly no nearby charged residues involved in the stabilization of the ProR TS. Moreover, the pK_a of proline in ProR may be estimated to be ca. 23.4, reflecting a reduction of more than 7 pK_a units when compared to the computed pK_a of 30.9 for proline in aqueous solution. This relatively high pK_a for Pro in the active site raises the question of why Cα-deprotonation occurs and not deprotonation of the ammonium of the zwitterionic Pro (p$K_a \approx 9.6$). Although this question was not directly addressed by PMF simulations, the answer is likely the tight interactions with His132 and Asp296, which prevent Pro from reorienting in a position enabling amine deprotonation. Indeed, during the course of the simulations, such a proton transfer was not observed.

An additional important finding in this study is the simplicity of the ProR mechanism (Scheme 1). Three additional mechanisms involving His132 and Asp296 as co-catalytic residues together with the Cys acid/base pair were investigated. These three pathways all yielded reaction barriers which are considerably higher than that of the classical mechanism, indicating that these mechanisms are not viable (Figure S4). Moreover, protonating either His132 or Asp296 or both, which is required

(72) Warshel, A.; Florian, J. *Proc. Natl. Acad. Sci. USA* **1998**, *95*, 5950–5955.

by mechanisms 2−4, compromises the H-bond network in the active site, yielding interactions which are substantially different to those in crystal structure with the transition state inhibitor PYC (Tables S7−S9). The free-energy profiles combined with the structural data suggest that these nonclassical mechanisms are incorrect.

Inspection of the PMF profiles for the various pathways yields considerable insight into the ProR active-site architecture. Indeed, analysis of the interaction energies in the classical reaction mechanism reveals a delicate balance of interactions. In the TS, the Pro carboxylate is bound in a *carboxylate hole* stabilized by a tight network of H-bonds, similar to that suggested for GluR[26] and the *oxyanion hole* in serine proteases. On the other hand, Cys130 and Cys300 only form a single H-bond each to backbone amides. Additionally, the nearby His132 and Asp296 both serve multiple noncovalent roles: In the L→D direction, His132 aids in the migration of the negative charge from Cys130 to Cys300, while Asp296 opposes the charge migration (Figure 6). In the D→L direction, His132 opposes migration of the negative charge from Cys130 to Cys300, while Asp296 aids charge migration (Figure 6). Moreover, the deprotonated forms of His132 and Asp296 avoids overstabilization of the Cys catalytic residues. In addition to the above roles, His132 and Asp296 play structural roles, firmly anchoring the substrate in position for reaction (Table 4). In the alternative more complex mechanisms suggested above, the delicate balance between regulating charge migration and destabilizing the Cys residues are violated. Indeed, in the three nonclassical mechanisms the Cys residues are overstabilized, rendering them ineffective catalytic bases. We therefore conclude that the deprotonated forms of His132 and Asp296 are crucial for the racemization charge migration and also play critical structural roles. However, these residues do not participate directly in the catalytic step. Nonetheless, we do not rule out their role in proton shuffling between Cys130 and Cys300 in the open form of the enzyme. These conclusions raise the question of the nature of the base responsible for the initial deprotonation of Cys130/300. Considering the pK_a value of ca. 8 for Cys130/300 in ProR and the fact that ProR operates at pH 8, water is most likely to play this role. Another possibility is the substrate, which might bind to the enzyme with its amine deprotonated.

In another extensively studied racemase, AlaR, PLP is employed as a cofactor. In a detailed study of AlaR it was found that the L-to-D-Ala isomerization in aqueous solution is a concerted process, similarly to the L-to-D-Pro isomerization. However, in the presence of the PLP moiety in aqueous solution the reaction mechanism involves a stable carbanion intermediate.[12,13,73,74] This carbanion intermediate is further stabilized by the enzyme environment in the AlaR-catalyzed reaction. Indeed, it was found that the pK_a shift due to the cofactor is 13.4 while the enzyme further reduces this value by 7.1. This latter value is similar to the effect of ProR on substrate acidity. The PLP cofactor reduces the free-energy barrier by 6 kcal/mol in aqueous solution compared to the uncatalyzed reaction, whereas the enzyme environment further reduces the barrier by 8 kcal/mol. Thus, in AlaR the total estimated computed catalytic effect of 14 kcal/mol is divided between the cofactor and the enzyme environment. We have previously shown that the PLP cofactor does not mainly serve as an electron sink in the AlaR catalyzed reaction. Rather, the effect of AlaR may be ascribed to a catalytic strategy of employing an unprotonated pyridine moiety in AlaR, yielding a conjugated substrate−cofactor with a net negative charge; C_α-deprotonation produces a doubly negatively charged moiety. This may be rationalized based on a simple solvent electrostatic description such as the Born model, $\Delta G^{solv}_{elec} = -q^2(1 - \varepsilon^{-1})/2r$, where q is the charge, ε is the relative permittivity of the medium (for a protein ca. 15),[75] and r is the radius of the solute cavity. Employing this model one obtains a change in electrostatic free energy of solvation upon deprotonation, $\Delta\Delta G^{solv}_{elec}$, of −135 kcal/mol for PLP−Ala, where a radius of 3.9 Å has been used (based on the computed volume enclosed by the solvent-accessible surface). In comparison, in ProR the zwitterionic substrate is neutral, and the solvation effect based on the Born model is −54 kcal/mol where a radius of 3.4 Å has been used. Thus, in AlaR the PLP cofactor enhances electrostatic stabilization by serving as a charge-carrier, reducing the net negative charge of the substrate.[76] Indeed, the active site in AlaR is composed of numerous charged residues which contribute considerably to catalysis.[12,13] Moreover, in AlaR distant charged residues play an important role. On the other hand, ProR primarily employs numerous polar, yet neutral residues, in stabilizing the transition state, which is obtained by a highly preorganized active site.

Conclusion

This work describes a hybrid classical and QM study of the ProR reaction. To elucidate the catalytic effect in ProR we employed a mixed QM/MM potential energy surface to describe the chemical aspects of the reaction, while employing a centroid path integral approach to describe nuclear QM effects. A main finding of this study is the similar mechanism in the aqueous solution deprotonation of proline and the enzymatic racemization catalyzed by ProR. In both cases, no stable intermediate is observed. Several possible mechanisms were investigated, and the most probable mechanism is one in which water or substrate deprotonates one of the catalytic Cys residues, without direct involvement of additional active site residues. In ProR, the reaction is found to be asynchronous concerted, in contrast to what is observed in the PLP-dependent enzyme AlaR, where a stable intermediate is observed. Additionally, the catalytic burden in ProR is borne by the enzyme environment alone, mainly via direct hydrogen-bonds to the substrate carboxylate moiety, while in AlaR the PLP cofactor contributes considerably to catalysis, in conjunction with numerous charged residues.

Acknowledgment. This work has been supported by a start-up grant from Bar-Ilan University and the Alon fellowship from the Council for higher education−planning and budgeting committee.

Supporting Information Available: Tables of Cartesian coordinates for model compounds and structural data for mechanisms 2−4, figures of intermolecular complexes, two-dimensional QM PMF for proton and deuteron transfer, one-dimensional PMF for mechanisms 2−4, pseudorotational plots, complete citations for refs 48 and 66, and a complete description of computational methods. This material is available free of charge via the Internet at http://pubs.acs.org.

JA900716Y

(73) Spies, M. A.; Toney, M. D. *Biochemistry* **2003**, *42*, 5099–5107.
(74) Spies, M. A.; Woodward, J. J.; Watnik, M. R.; Toney, M. D. *J. Am. Chem. Soc.* **2004**, *126*, 7464–7475.
(75) Löffler, G.; Schreiber, H.; Steinhauser, O. *J. Mol. Biol.* **1997**, *270*, 520–534.
(76) Here, we have assumed that the electrostatic free energy of solvation upon protonation, $\Delta\Delta G^{solv}_{elec}$ is similar for the catalytic bases in ProR (Cys) and AlaR (Tyr and Lys).